Cost-effective bioprocess design for the manufacture of allogeneic CAR-T cell therapies using a decisional tool with multi-attribute decision-making analysis

Michael J. Jenkins, Suzanne S. Farid*

Department of Biochemical Engineering, University College London, Gower Street, London, WCIE 6BT, UK

ABSTRACT

Reimbursement pressures have resulted in an increased awareness of the importance of estimating and improving manufacturing costs for cell therapy products. This work describes the development and application of a decisional tool capable of computing the manufacturing costs for an allogeneic CAR-T cell bioprocess. The tool was used to facilitate a comparison of the impact on cost of goods (COG) from the use of different process technologies including T-flasks, gas permeable vessels, rocking motion bioreactors, an integrated processing platform, MACS purification and spinning membrane filtration technology. Seven different process flowsheets were compared and the economic drivers of manufacturing costs were analysed. COG per dose values were compared against a specified target selling price (TSP) to understand the feasibility of achieving a target COG as % TSP. Finally, a multi-attribute decision-making (MADM) analysis was conducted in order to allow preference of process design to be determined on the basis of qualitative and quantitative operational attributes, rather than COG alone. The flowsheet containing rocking motion bioreactors, spinning membrane filtration technology and a MACS purification platform was found to result in the lowest COG value. The MADM analysis indicated that this was also the preferred flowsheet when qualitative operational attributes were also considered. Furthermore, process attributes such as viral transduction efficiency and electroporation efficiency were found to be key process economic drivers.

© 2018 The Authors. Published by Elsevier B.V. This is an open access article under the CC BY license (http://creativecommons.org/licenses/by/4.0/).

1. Introduction

Many chimeric antigen receptor (CAR) T cell therapies currently in development are autologous. This has been reflected by the focus of the majority of process design commentaries and analyses in this area to date [e.g. 1–3]. However, recent advances have allowed the silencing of T cell receptor (TCR) expression on T cells derived from normal healthy donor so as to avoid alloreactivity [4]. This has paved the way for the development of allogeneic CAR-T cell therapies. A major advantage of an allogeneic CAR-T therapy is that it could be used as an off-the-shelf treatment in acute oncology cases if a patient is either too ill to provide their own T-cell sample, or if they cannot provide the requisite number of T-cells required for the manufacture of an autologous product. Further to this, universal cell therapies align with traditional scale-up strategies and greater economies of scale could be realised with such a product. Allogeneic CAR-T cell therapies have the potential to enable more affordable treatments when compared to their autologous counterparts that are estimated to command a price bracket of US$150k – US$650k [5–7]. Whilst allogeneic CAR-T cells may be able to provide solutions to cost of goods challenges currently observed in relation to autologous products, the clinical safety and efficacy of the approach are still being explored.

At the forefront of current commercial challenges to cell therapies is the production of cells at a relevant quantity and quality to support their function. Traditional, planar technologies that offer reliable tools for laboratory-based protocols are labour-intensive and do not lend themselves to large scale, allogeneic processes. The majority of dose sizes reported for CAR-T cell therapy products are estimated to be on the order of $10^7 - 10^9$ cells, although full dose ranges vary from $10^4 - 10^{12}$ cells [8].

Further to this, technologies used for the concentration of T-cell populations following cell culture have also improved. Spinning filter membrane technologies (e.g. Lovo Cell Processing System (Fresenius Kabi, Lake Zurich, IL, USA)) [9] and fluidised bed centrifuge systems (e.g. kSep (Sartorius, Göttingen, Germany)) [10],

along with integrated systems mentioned above where the cell culture chamber also acts as a centrifuge, now offer efficient means of cell concentration in a closed environment. This represents a welcome shift from more conventional, planar technologies that do not offer the process control, flexibility, or potential for scale-up associated with modern technologies. Despite these advances, cost of goods (COG) associated with the production of CAR-T cell therapies are still a major challenge facing products of this nature.

Advances in technologies have seen platforms such as the following being evaluated in cell therapy bioprocessing applications: gas-permeable vessels (e.g. G-Rex (Wilson Wolf, New Brighton, MN, USA)) [11], rocking motion bioreactors (e.g. Xuri Cell Expansion System (GE Healthcare, Chicago, IL, USA)), and contained, integrated bioprocess platforms (e.g. CliniMACS Prodigy (Miltenyi Biotec, Bergisch Gladbach, Germany)) [1]. Further to this, technologies used for the concentration of T-cell populations following cell culture have also improved. Spinning filter membrane technologies [9] (e.g. Lovo Cell Processing System (Fresenius Kabi, Lake Zurich, IL, USA)) and fluidised bed centrifuge systems (e.g. kSep (Sartorius, Göttingen, Germany)) [10], along with integrated systems mentioned above where the cell culture chamber also acts as a centrifuge, now offer efficient means of cell concentration in a closed environment. This represents a welcome shift from more conventional, planar technologies that do not offer the process control, flexibility, or potential for scale-up associated with modern technologies. Despite these advances, cost of goods (COG) associated with the production of CAR-T cell therapies are still a major challenge facing products of this nature.

The use of decisional tools can prove useful in the identification of cost-effective bioprocess designs and equipment sizing regimes. Further to this, decision-support tools and cost of goods (COG) models offer a means to capture resource requirements and the process economics associated with different bioprocess designs in order to aid process development decisions early on in product development. At the time of writing there is a small, but growing number of this type of analysis that has been applied to cell therapy bioprocesses. Commercially available flowsheeting software has been used to evaluate the relative economic potential of iPSC-derived cell bioprocess designs [12]. The use of bespoke decisional tools to aid cost-effective process design has also been demonstrated by numerous studies. The use of manual versus automated cell culture platforms during the production of patient-specific iPSC-derived cell populations across a variety of scales has been considered [13]. Furthermore, the use of a combined experimental and economic approach has identified the most cost-effective process platform for purification of hiPSC-derived retinal progenitor cells (RPCs) as part of the manufacture of an autologous cell therapy product; this approach also highlighted economic and feasibility constraints of currently available purification technologies [14]. For mesenchymal stem cells (MSCs), published studies have focused on the impact of different potential commercial dose-demand scenarios and their impact on the scale at which microcarriers in single-use bioreactors (SUBs) become preferable to planar-based technologies from an economic perspective [15,16], and on the optimal single-use scalable downstream processing technologies for volume reduction [17]. Further to this, Hassan et al. [18] showed how a decisional tool could be used to evaluate the effect of process changes during different phases of clinical development on the long-term profitability of a project.

Multi-attribute decision-making (MADM) analysis provides a mechanism for qualitative, as well as quantitative attributes of a solution to a bioprocess design problem to be evaluated. MADM requires that all attributes are considered across an equivalent measurement scale, this is usually done by converting all attributes to dimensionless units on a finite rating scale. This method therefore allows preference decisions to be made on the basis of multiple attributes for an array of different problem solutions [19]. MADM analyses have previously been applied within various decision support tools in the biopharmaceutical sector in order to evaluate bioprocess designs on the basis of operational, environmental, and economic attributes [20,21].

To date, no economic analyses or decisional tools relating to CAR-T cell therapy bioprocessing have been published. CAR-T cell therapies demand a unique production process. T-cells must be activated and be genetically manipulated in order to express a CAR protein; the material required to do this is usually transduced via a viral vector. Further to this, allogeneic CAR-T cell therapies require an additional unit operation in order to silence genes causing the expression of T-cell receptors (TCRs), which could mediate graft-versus-host disease (GvHD) in recipient patients.

This study describes the development and application of a decisional tool that has been designed to capture the resource requirements and COG associated with different bioprocess flowsheets put forward for the production of an allogeneic CAR-T cell therapy for the treatment of haematological malignancies. This paper evaluates the use of different types of cell culture vessels (rocking motion bioreactor, gas permeable vessel, and tissue culture flasks) when used in conjunction with a variety of different devices for media removal (fluidised bed centrifuge, spinning filter membrane, integrated bioprocess platform based on continuous centrifugation, automated media removal pump). Additionally, the tool highlights process economic drivers associated with each bioprocess flowsheet. Scenario analyses are used to probe the effects of process improvements on COG as a percentage of target selling price. Finally, multi-attribute decision making (MADM) analysis is applied to quantitatively evaluate different allogeneic CAR-T cell therapy bioprocess flowsheets from both financial and operational perspectives. This is the first time such an analysis has been applied to the production of an allogeneic CAR-T cell therapy.

2. Tool description

A decisional tool was developed in order to evaluate different bioprocess flowsheets and process technologies associated with the manufacture of an allogeneic CAR-T cell therapy from an economic and operational perspective. The tool comprises a bioprocess economics model, an information database, and a multi-attribute decision making (MADM) module. The tool was implemented in Microsoft Excel (Microsoft Corporation, WA, USA) and Visual Basic for Application (VBA) (Microsoft Corporation). The tool architecture is described in Fig. 1. The bioprocess economics model was used to calculate quantitative data in order to compute the financial attributes (COG, fixed capital investment) considered in the MADM analysis. The stochastic MADM analysis was configured to assess the impact of uncertainty and variability in the weightings and ratings of financial and operational attributes on what was deemed to be the optimal process design.

2.1. Bioprocess economics model

The bioprocess economics model used in this case study is based upon that described in Jenkins et al. [13]. The model makes use of equipment sizing calculations, mass balance equations and cost computations (based on key resource requirements) in order to provide an economic evaluation of the different technologies that were available for use in different unit operations within the bioprocess. The bioprocess economics model utilised data stored in the information database pertaining to the technologies evaluated within this study, as well as basic bioprocess assumptions such as the costs of raw materials and labour, and bioprocess unit operation yields.
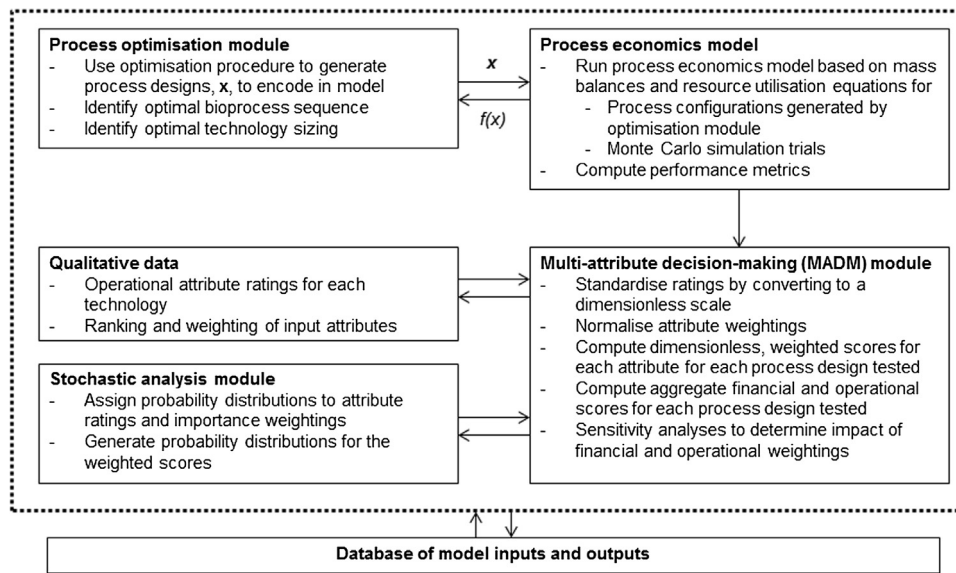
Fig. 1. Decisional tool framework used within this study. Information from the process economics model is fed into the MADM component of the tool, along with qualitative data obtained from responses to surveys completed by industry experts. Data was handled by the database in the same manner as previously described.

Key input parameters for the bioprocess economics model include the annual demand, d, and the dose size, s. Briefly, the bioprocess economics model was implemented to compute the COG per dose for a given process flow-sheet (or design) as follows:

$$\text{COG per dose} = \frac{c_{mat} + c_{lab} + c_{dep}}{d} \tag{1}$$

where c_{mat}, c_{lab} and c_{dep} represent the annual cost of materials, labour, and the cost of fixed equipment depreciation respectively. Material, labour, and depreciation costs are functions of the technologies selected within a given bioprocess design.

2.2. Multi-attribute decision making methodology

Industry experts were asked to rate different process technologies on a scale of 1–10 for the operational attributes considered for each candidate technology tested by the tool. These ratings made up the qualitative data described in Fig. 1.

2.2.1. Additive weighting technique

In this work, the additive weighting technique was applied to a multi-attribute bioprocess design problem where economic and operational attributes were considered. An aggregate score, W, for each alternative, *j*, was computed by multiplying the normalised rating for each attribute included in the analysis by the weight (representing the importance of each attribute) assigned to each attribute; these products were then summed over all the attributes (Yoon and Hwang, 1995). This can be represented mathematically as:

$$W_j = \sum_{i}^{n} w_i r_{ij} \tag{2}$$

where w_i = normalised weight assigned to attribute i
r_{ij} = dimensionless rating of attribute i for alternative j

The additive weighting technique relies on assigning weightings to all attributes; these weightings are relative to the importance of each attribute within a given field. A greater weighting that an attribute is given, the more important it is. Weightings were converted to a 0–1 scale in order to allow an aggregate score to be computed.

Prior to computation of the aggregate score using Eq. (2), each alternative (*j*) had to be assigned a rating (x) for each attribute (i), which then had to be standardised. Economic attributes (e.g. COG, FCI) were calculated using the bioprocess economics model. Operational attribute ratings, and their relative importance, were collated from responses to a survey delivered to industry experts.

Different types of attributes were assigned ratings based on a number of different dimensions and measurement units. All attribute ratings were therefore standardised by converting them to a dimensionless, 0–100, scale. Standardisation was achieved by giving each attribute a rating that was a fraction of a feasible range of the best and worst attainable value for any given attribute. The dimensionless rating for each attribute, r_{ij}, was therefore calculated as:

$$r_{ij} = \left| \frac{x_{ij} - x_{i\,worst}}{x_{i\,best} - x_{i\,worst}} \right| \tag{3}$$

where x_{ij} = rating value assigned to alternative *j* for attribute i
$x_{i\,best}$ = best attainable value for attribute i
$x_{i\,worst}$ = worst attainable value for attribute i

2.2.2. Weighted financial and operational scores

The relative importance of the total weighted economic and operational scores were captured using combination ratios, whose sum is equal to one. Overall aggregate scores for each alternative solution, W*j*, were therefore calculated as follows:

$$W_{j\,overall} = \left(\frac{\sum_{i=1}^{n} r_{ij\,economic}}{n} * R_1 \right) + \left(\frac{\sum_{i=1}^{n} r_{ij\,operational}}{n} * R_2 \right) \tag{4}$$

where R_1 = economic combination ratio
R_2 = operational combination ratio
$R_1 + R_2 = 1$

2.2.3. Stochastic additive weighting

Input variables in MADM analysis include weightings assigned to each attribute and the ratings assigned to each attribute for each process strategy tested using the analysis. In order to capture the uncertainty in ratings and importance weightings assigned

Table 1
Attributes considered in the MADM analysis, along with their respective weightings and probability distributions.

Attribute Category	Attribute Name	Importance Rank	Weighting
Financial	FCI	1	Uniform (90,100)
	COG per dose	2	Uniform (40, 100)
Operational	Process control	1	Uniform (85, 95)
	Process containment	2	Uniform (65, 75)
	Ease of scale-up	3	Uniform (45, 65)
	Ease of validation	4	Uniform (30, 60)
	Validation effort	5	Uniform (10, 40)

to each attribute considered within the MADM analysis, probability distributions were assigned to a) the ratings assigned to each attribute for each process design evaluated within the MADM analysis (Table 1) and b) the importance weightings assigned to each attribute considered in the MADM analysis (please see results section). The probability distributions were then used as the inputs for a Monte Carlo simulation in order to characterise the variability in the weights and ratings of the financial and operational attributes. This allowed for more informed decision making, and the level of confidence associated with such a decision [22]

The Monte Carlo method requires estimates of probability distributions for uncertain input parameters associated with the MADM analysis; these probability distributions are assigned to key process parameters. A sample outcome is randomly generated by assigning a value to each parameter tested in the simulation according to its specific probability distribution. This process was repeated 1000 times in order to generate frequency distributions of simulation outcomes. The output distributions of the Monte Carlo experiment can then be used to determine the probabilistic properties associated with the key performance metrics of a bioprocess design or manufacturing strategy.

2.3. Sensitivity analysis

A sensitivity analysis was carried out in order to identify key process economic drivers associated with the process. Process input parameters were varied by arbitrarily decided upon values of ±15% of their original value in order to assess their impact on COG. For example, when the base case viral transduction efficiency, 70%, was varied by ±15% the worst case value was 59.5% and the best case value was 80.5%.

3. Case study set-up

3.1. Tool application

The decisional tool was applied to a case study designed to evaluate the use of different process technologies for the manufacture of an allogeneic CAR-T cell therapy product. At this time, and with limited clinical experience, we estimated that CAR-T cell therapy dose sizes will vary depending on the target indication from $\sim 10^4$–10^{12} cells per Kg, with the majority of those tested in the region of 10^6 – 10^9 cells per dose [8]. The annual demand is also likely to vary dependent on target indication; rare haematological malignancies may only warrant an annual market size numbering in the low hundreds, whereas more common indications may require thousands of doses per year. In this instance, a target dose size of 10^8 target cells and an annual demand of 1000 doses was set as the base case scenario as these values are believed to be the near the midpoint. The effects of dose size and annual demand on COG were analysed using the bioprocess economics model; dose sizes ranging from 10^7 to 10^9 total cells and annual demands rang-

Table 2
Cell culture technologies considered within this case study and their associated performance and cost parameters.

Equipment Type	Name	Volume (L)	Working culture volume (L)	Minimum Utilisation	Maximum Cell Density	Single-use vessel costs	Fixed equipment costs	Perfusion rate
Rocking Motion Bioreactor (RMB)	50 L RMB	50	25	20%	3.50E+07	$793.75	67,500	30% –100% of WV depending on cell concentration
	20 L RMB	20	10	10%	3.50E+07	$778.13	67,500	
	10 L RMB	10	5	10%	3.50E+07	$765.63	67,500	
	2 L RMB	2	1	30%	3.50E+07	$739.06	67,500	
Planar culture flask (CF)[b]	L-5	1.6	1.6	100%	4.00E+06	$198.44	N/A[a]	Media addition based on cell population
	L-2	0.8	0.8	100%	4.00E+06	$183.59	N/A[a]	
	L-1	0.3	0.3	100%	4.00E+06	$73.57	N/A[a]	
	T225	0.05	0.05	100%	4.00E+06	$8.64	N/A[a]	
Gas permeable vessel (GPV)[b]	GPV500	5.5	5.5	10%	4.00E+06	$951.50	15,000[a]	Media addition based on cell population
	GPV100	1.1	1.1	10%	4.00E+06	$190.30	15,000[a]	
	GPV10	0.1	0.1	10%	4.00E+06	$156.48	15,000[a]	
Integrated bioprocess platform (INT)	INT	3.8	0.65	4%	3.50E+07	$2512.00	235,500	N/A

WV = working volume.
[a] Maximum cell density obtained from personal communications with Pfizer Inc., unpublished process development data.
[b] Indicates that additional fixed equipment such as incubators and BSCs are required – please see table 4 for details on this equipment.
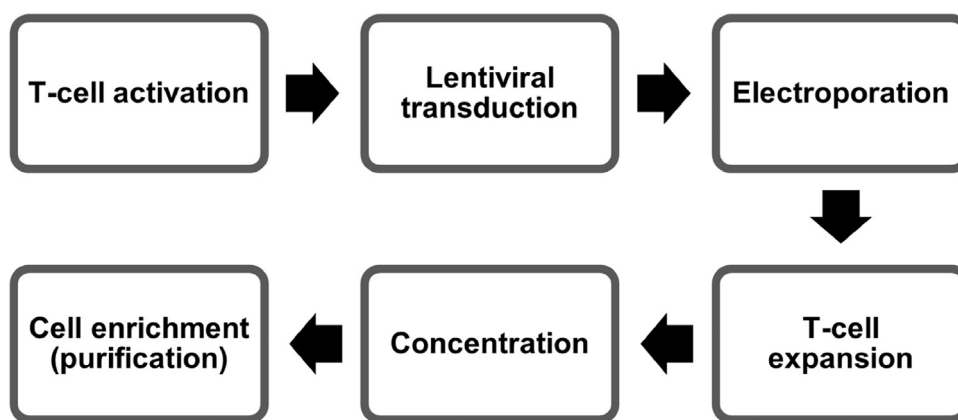
Fig. 2. The process flowsheet considered within this case study for the production of an allogeneic CAR-T cell therapy.

ing from 500 to 5000 doses were tested as the extremes using the model.

The bioprocess economics model was used to compute COG and FCI requirements for different bioprocess designs; these economic parameters were then combined with the operational ratings for different technologies in order to create a MADM rating for each process design tested using the tool.

3.2. Process overview

The bioprocess in question is outlined in Fig. 2, where it is broken down into unit operations. This process flowsheet differs from a typical autologous process in that additional unit operations in the form of electroporation and purification are required. Electroporation is utilised in order to transfer genetic material that silences the genes causing expression of T-cell receptor $\alpha\beta$ (TCR). TCR$^-$ cells avoid GvH reactions [4]. Purification, or enrichment, of TCR$^-$ cells at the end of the bioprocess is required (Fig. 2) in order to attain a targeted level of purity of TCR- cells amongst the total cell population that forms the therapy in this instance.

Three categories of cell culture technology were tested within the model so as to reflect the choices of available technologies on the market; tissue culture flasks (TCFs), including T-flasks and manually operated stacked culture vessels; gas permeable vessels (GPVs); and finally rocking motion bioreactors (RMBs). Key input parameters regarding these technologies are summarised in Table 2.

The concentration technologies tested included fluidised bed centrifugation (FBC), spinning membrane filtration (SFM), automated media removal (AMR) – to be used in conjunction with

GPVs only – and finally an integrated process technology offering the potential for cell culture, concentration and purification in a contained, all-in-one platform (integrated process platform (INT)). Key input parameters pertaining to concentration technologies can be found in Table 3, where data is also available for the purification technologies considered in this study; namely a standalone magnetic-activated cell sorting platform (MACS) and a MACS platform within the integrated process platform technology described above. Where the integrated process platform is used for purification, the platform was also assumed to be used for concentration as well. Static cell culture bags were assumed to support transduction and activation unit operations, whereas electroporation was carried out using the AgilePulse machine (BTX, MA, USA).

A base case viral transduction efficiency of 70% was selected as it is within the range reported in literature [23], as well as consistent with values seen during process development work carried out by Pfizer (data not shown). Within the sensitivity and scenario analyses, viral transduction efficiencies ranging from 50% to 90% were used. Key process and cost assumptions associated with the bioprocess, including reagent and material costs, labour costs, fixed capital equipment costs and specific process yields can be found in Table 4. Table 5 illustrates the 7 different process configurations tested by the model; different process configurations are described by their Flowsheet Number (1 to 7) from this point forward.

The attributes tested within this case study fell into two categories: financial and operational. Attributes and their rank, in terms of importance, were determined via consultation with industry experts. The final list of attributes, the category to which they are assigned, and the importance weighting assigned to each attribute are listed in Table 1. Weightings were assigned probability

Table 3
Cell concentration and purification (cell enrichment) technologies considered in this case study and their associated cost and performance parameters.

Concentration Technologies							
Equipment Type	Abbreviation	Maximum input	Maximum cell density	Viable cell yield	Target cell yield	Consumable costs per run (US$)	Fixed equipment costs (US$)
Fluidised bed centrifugation	FBC	114L	N/A	80%	N/A	1,800	281,000
Spinning filter membrane	SFM	7.2L	1.6	85%	N/A	537	79,500
Integrated bioprocess platform	INT	3.5×10^{10} cells	0.65	86%	N/A	3,000	235,500

Purification Technologies							
Equipment Type	Abbreviation	Maximum input	Maximum cell density	Viable cell yield	Target cell yield	Consumable costs per run (US$)	Fixed equipment costs (US$)
Stand-alone immuno-affinity purification	MACS	3.5×10^{10} cells	N/A	95%	80%	2,217	55,000
Integrated bioprocess platform-based immune-purification	INT	3.5×10^{10} cells	N/A	95%	80%	3,000	235,500

Table 4
Key cost assumptions used within the bioprocess economics model.

Cost Parameter		Value
Media & Reagents		
	Activation beads	US$454/mL
	Electroporation buffer	US$785/L
	TALEN plasmid	US$6,500/mg
	Expansion media	US$300/L
	SFM buffer	US$100/L
	FBC buffer	US$80/L
	INT concentration buffer	US$300/L
	Purification buffer	US$2,157/L
	Purification reagents	US$3636 per 10^{10} cells
Labour		
	Operator cost	US$120,000/yr
Fixed Equipment		
	Incubator	US$27,000
	BSC	US$12,000
	AgilePulse electroporator	US$32,400

Table 5
Flowsheet configurations considered within the bioprocess case study (equipment sizes shown where relevant).

Flowsheet Number	Cell culture	Cell concentration	Purification (cell enrichment)
1	RMB (10 L)	FBC	MACS
2	RMB (10 L)	SFM	MACS
3	RMB (10 L)	INT	INT
4	GPV500	AMR	MACS
5	L-5	FBC	MACS
6	L-5	SFM	MACS
7	L-5	INT	INT

distributions to capture the uncertainty in these values. These distributions were utilised in the stochastic MADM analysis. The COG and fixed capital investment associated with each process design were selected as the financial measures used in the MADM analysis. The COG is a key quantitative measure of the cost-effectiveness of a bioprocess, and has therefore been included in this analysis. FCI represents the upfront costs required to build a new facility fit for housing a bioprocess. Typically, many companies involved in cell therapy product development are academic spin outs and SMEs [24]. Many of these players are likely to view the upfront costs associated with a process design as a key factor to consider with regards to bioprocess design. Equally, larger companies may view high FCI costs as a significant risk associated with a particular project; FCI was therefore included in the MADM analysis.

Qualitative attributes, such as process control, and process containment are vital to the robustness and reproducibility of cell therapy bioprocesses. These are two areas upon which product quality is dependent. Furthermore, ease of scale-up and ease of operation are important attributes to capture in the MADM analysis. For instance, technologies such as automated media removal are not commonly associated with high fixed equipment costs, unlike fluidised bed centrifuge and spinning membrane filtration units. It is important to translate these qualitative trade-offs into quantitative measures within the MADM analysis. The likely validation effort supported by different technologies is also important to capture. For example, technologies which rely on manual operators and are therefore more prone to human error and may require additional validation studies in order to prove the consistency of product quality over multiple production lots.

4. Results and discussion

This section discusses insights from the process economics analysis of alternative whole bioprocess flowsheets for allogeneic CAR-T cell therapies. It provides a breakdown of the COG categories for each flowsheet as well as the bottlenecks and cost drivers in each case. The cost analysis is extended using a stochastic MADM analysis to weigh up the financial and operational attributes of each flowsheet.

4.1. Bioprocess economic model results

Fig. 3 shows the relative COG per dose values, broken down into constituent cost categories, associated with each bioprocess flowsheet. Whilst the optimal process flowsheet (Flowsheet 2), in terms of COG, is highlighted in Fig. 3, COG differences of <5% are considered insignificant due to the margin of error associated with the COG model. Percentage values above each column in the chart refer to the COG difference relative to the optimal flowsheet.

Flowsheets 1–4, which all involve rocking motion bioreactors or gas-permeable vessels as the cell culture platform, all lie within 10% of one another (Fig. 3). However, Flowsheets 5–7, for which tissue culture flasks are the cell culture platform, all have a COG value at least 20% larger than the Flowsheet 2 (optimal COG). Fig. 3 shows that the major difference in the COG between flowsheets including tissue culture flasks compared to those where cell culture is supported by rocking motion bioreactors and gas-permeable vessels is the labour costs. Flowsheets 5–7 require seven, seven and six cell culture units respectively; this is compared to one unit for Flow-
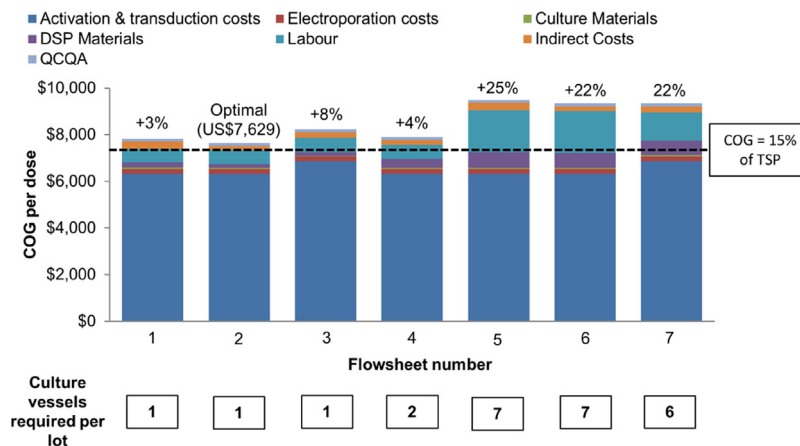
Fig. 3. Stacked column chart displaying COG per dose made up of its constituent parts for each process flowsheet. Numbers on the x-axis refer to the process flowsheet numbers introduced in Table 5. The dashed line intersecting the y-axis at US $7500 represents the modelled COG value that is equal to 15% of target selling price. Panels inset below the x-axis indicate the number of culture vessels required per lot for each process design. The technologies used in each flowsheet deign are provided in Table 5.
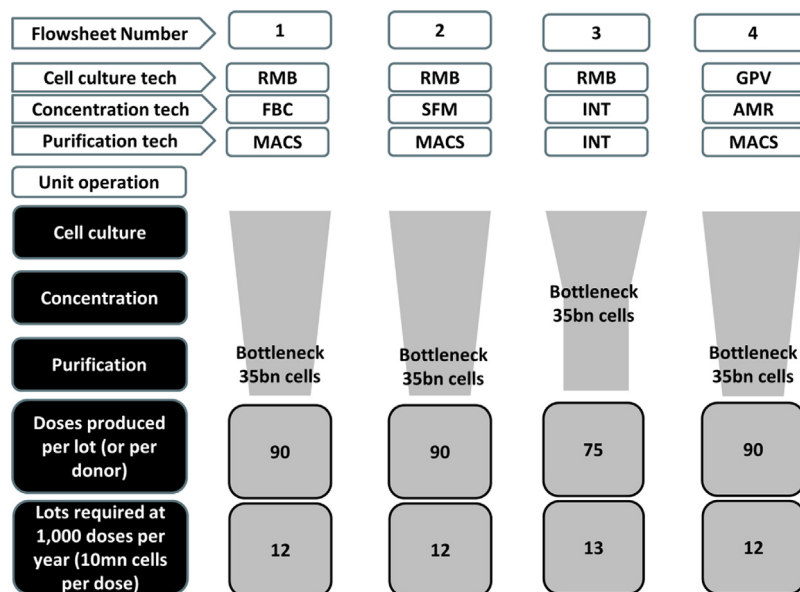
Fig. 4. Schematic and inset panels summarising the capacity bottlenecks, doses produced per lot, and number of lots required per annum for the process flowsheets with the lowest COG per dose values. Unit operations are shown in the panels on the left of the figure. The capacity bottleneck (in terms of number of cells that can be handled) is overlaid for each process flowsheet and is positioned according to the unit operation where this occurs. This label indicates the unit operation whereby the number of cells that can be handled by the technology used within a given flowsheet is the limiting factor on the scalability of the process design. The technologies used in each flowsheet deign are provided in Table 5.

sheets 1–3 and to two units for Flowsheet 4 (table insert, Fig. 3). Hence, more operators are required for flowsheets that include tissue culture flasks; this is reflected in the increased labour costs. This reinforces the greater scalability of rocking motion bioreactors compared to tissue culture flasks.

Capacity limitations and their consequences on lot size and number of lots required are illustrated by the capacity bottleneck schematics and inset panels for the four highest ranked flowsheets (determined by COG) in Fig. 4. Flowsheet 3, where INT is used, can produce 78 doses per lot; this is compared to 90 doses per lot for Flowsheets 1, 2 & 4, where fluidised bed centrifuge, spinning membrane filtration and automated media removal are the respective concentration technologies. This means that 13 lots per year are required if integrated process platform is used for cell concentration, as opposed to 12 if other technologies are considered. This is due to the reduced cell concentration capacity offered by the integrated process platform as compared to other platforms considered in the study. Therefore, because VT costs are calculated on a 'per lot' basis, Flowsheets 3 and 7 result in increased viral transduction costs compared to other flowsheets (Fig. 3).

When the integrated process platform is not considered for cell concentration, the capacity of the purification platforms is the limiting factor on the number of doses that can be produced per lot (Fig. 4).

A target selling price (TSP) of US$50,000 was selected based on costs for marketed cellular therapies being in the range of ~US$1000 to US$100,000 [25]; an approximate midpoint of these values was chosen for calculations in this case study. At the time of writing, two autologous CAR-T cell therapies have been approved by the FDA; Kymriah[TM] or tisagenlecleucel-t (Novartis, Basel, Switzerland) for acute lymphoblastic leukemia and Yescarata[TM] or axicabtagene ciloleucel (Gilead, CA, USA) for diffuse large B-cell lymphoma. Prices for these therapies in the US are listed as US$475,000 and US$373,000 respectively, in line with early estimates that predicted prices would be in the several hundred thousand dollar range for autologous CAR-T cell products [5–7]. In the biologics industry typical values for COG as % sales are reported from 15% to 40% in order to recover R&D, sales and marketing costs

[26]. In order to maximize the sensitivity model, a figure on the very low end of this range (15%) was selected [15,17,26], which translates in to a COG target of US$7500 in this case study.

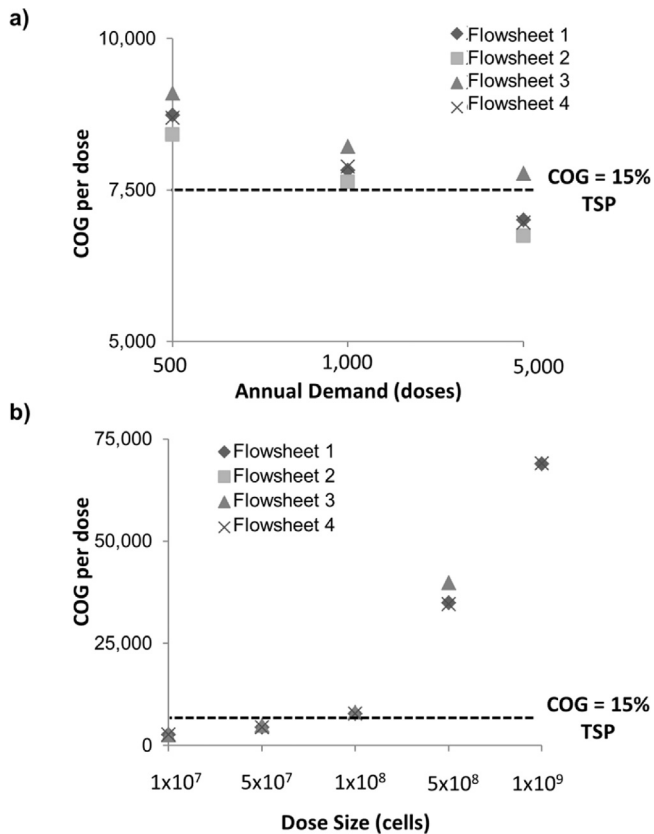### 4.2. Effect of dose size and annual demand on COG

Different annual demands and dose sizes were investigated in order to test their effect on the COG of the four highest ranked Flowsheets (according to COG), and whether the target of a COG value of less than 15% of target selling price (TSP) was realistic across these scenarios.

The trend dis played within Fig. 5a, whereby COG per dose decreases as the annual demand increases is consistent with economies of scale that are associated with scale-up of allogeneic cell therapies; reductions in labour costs and the distribution of FCI costs across a larger annual demand are the causes of this. This is concurrent with both current opinion in the field of cell therapy bioprocessing and findings of previous analyses [15].

At a the highest annual demand of 5000 doses per year, Flowsheet 2 still exhibits the lowest COG value; this equates to ~13% of TSP as shown by the scatter plot in Fig. 5a – which displays COG values for the four flowsheets across the different annual demands. Flowsheets 1 and 4 also exhibit COG values that are less than 15% of TSP. Flowsheet 3 exhibits COG > 15% TSP; this is due to the increased viral transduction costs associated with this Flowsheet that are discussed in Section 4.1.

At annual demands of 500 doses per annum all four process flowsheets tested resulted in scenarios where COG > 15% of TSP. As with other demands that were analysed, Flowsheet 2 resulted in the lowest COG figure, which was approximately 17% of TSP. Similarly, Flowsheet 3 proved to have the highest COG, whereby COG is equal to ~19% of TSP. At all annual demands the COG for Flowsheet 1 and Flowsheet 4 fell within 1% of each other's value, indicating that there is no significant difference between these process designs from a COG perspective.

Fig. 5b shows that changes in COG associated with changes in dose size are more dramatic when compared with those associated with changes in annual demand (Fig. 5a). For dose sizes less
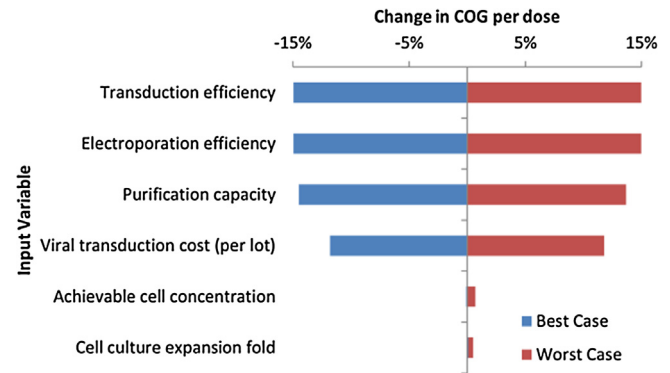
Fig. 6. Tornado charts showing the effect that a ±15% change in key parameters has upon the COG per dose in terms of a percentage change. Best case values, whereby COG per dose decrease relative to the base case are shown to the left of the y-axis (negative values). Worst case values are shown to the right of the y-axis (positive values).

Fig. 5. Scatter plots indicating the effect of **a)** annual demand and **b)** dose size on the COG per dose for Flowsheets 1-4. Dashed lines on the plots that intersect the x-axis at US$7500 indicate the modelled COG value that is equal to 15% of target selling price.

than 10^8 target cells, a COG per dose value of <=15% of sales is achievable. For dose sizes of 5×10^8 and above, manufacturing costs exceed far beyond this value; as high as 170% of TSP in the case of Flowsheet 3 at a dose size of 10^9 cells. As dose size increases, so too does the number of lots required per year. This is because number of doses produced per lot decreases as dose size increases. The dramatic rises in COG associated with increase in dose size observed in Fig. 5b can be attributed to viral transduction costs, which are carried out on a 'per lot' basis. Owing to the fact that large dose sizes result in COG that greatly exceed the 15% of TSP target set, therapies for indications that require increased dose sizes may prove challenging from a reimbursement perspective. The sales price achieved by a cell therapy will likely be determined by its quality and efficacy relative to currently available comparators, and key performance indicators as described by health technology assessments (HTAs).

4.3. Sensitivity analysis: identification of key process economic drivers

The tornado charts in Fig. 6 illustrate the changes in COG that variations in input parameters effect. Transduction efficiency and electroporation efficiency proved to be the greatest economic drivers associated with this bioprocess, each resulting in a 30% swing in COG when altered by ± 15%. Both these parameters have a direct impact on the number of target cells that can be produced per lot; this is why they effect such a major change in COG when varied. Purification technology capacity was ranked third in the sensitivity analysis. Fig. 4 shows that the capacity of currently available purification technologies causes a capacity bottleneck; therefore, an increase in this parameter would increase achiev-

able lot sizes and thus reduce the number of viral transduction processes required to satisfy annual demands. The tornado charts show that the COG per lot of viral transduction has a significant impact on COG; it is the parameter ranked fourth in the sensitivity analysis. This is to be expected given the fact that the cost of viral transduction dominates the COG breakdowns shown in Fig. 3.

Finally, it is of note that variations in the cell culture expansion fold have little impact on COG. This is in contrast to the data presented in previous studies related to human cell culture [13] whereby cell culture expansion fold (expressed as number of expansion stages required) was a key process economic driver. However, in this instance it has little effect because of the DSP capacity bottlenecks referred to in Section 4.1; a higher expansion fold may create incremental reductions in material costs associated with cell culture, but will not impact on the number of doses that can be produced per lot.

Downstream processing across multiple units in parallel was not initially permitted during this study; this is consistent with previous analyses in this area where historically this has been considered undesirable at large scale due to validation concerns [15,18]. However, parallel downstream processing operations, whereby multiple DSP units are used and the process is pooled at the end of purification or concentration are now being considered in the sector given existing capacity constraints of units. In order to accommodate this, an equipment sizing evaluation was carried out in order to estimate the effects of parallel downstream processing on capacity bottlenecks within the bioprocess. This is shown in Fig. 7. The results presented in Fig. 7 indicate that purification would no longer be the bottleneck or restricting factor on the scalability of the bioprocess and that the number of doses produced per lot would range from 311 to 334 as opposed to 75 to 90 (Fig. 4) as was previously described. This is because the performance of the cell culture operation is now the limiting factor; maximum cell yield from this operation is 150bn cells per lot. Interestingly, Flowsheet 3, containing the integrated process platform would now allow for the greatest number of doses to be produced per lot; previously this Flowsheet produced the smallest number of doses per lot. Additionally, the number of lots required per year is reduced from 12 (Fig. 4) to four (Fig. 7). Viral transduction costs are calculated on a per lot basis and Fig. 4 illustrates that they account for a significant proportion of overall COG. It is therefore conceivable that permission of the use of downstream processing units (DSP) units in parallel could significantly reduce COG per dose; although additional capital expenditure on additional DSP units will also be required to facilitate this scenario. Overall, this analysis suggests that the pro-
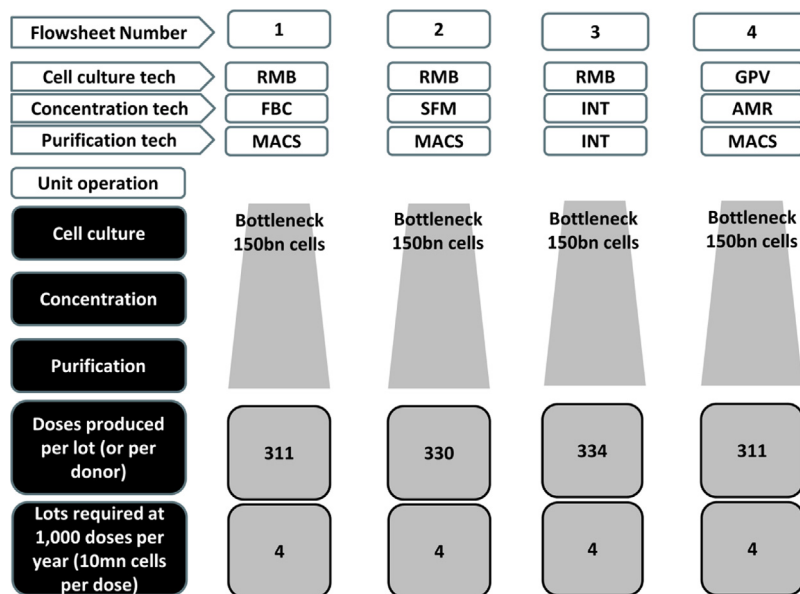
Fig. 7. Schematic and inset panels summarising the capacity bottlenecks, doses produced per lot, and number of lots required per annum for the process flowsheets where multiple DSP units are permitted. Unit operations are shown in the panels on the left of the figure. The capacity bottleneck (in terms of number of cells that can be handled) is overlaid for each process flowsheet and is positioned according to the unit operation where this occurs. This label indicates the unit operation whereby the number of cells that can be produced due to process limitations is a constraining factor on the scalability of the bioprocess. The technologies used in each flowsheet deign are provided in Table 5.

cess can be de-bottlenecked at the purification stage of the process in this scenario.

4.4. Scenario analyses

Based on the results of the sensitivity analysis described in Section 4.3, scenario analyses were carried out in order to identify process improvements or cost reductions necessary to achieve a target COG value. In these analyses, the impact of simultaneously varying two or more key economic drivers upon the COG was measured. This allowed the identification of the amount by which current process yields and efficiencies, or process costs, need to change in order to hit a target COG. Analyses were performed using Flowsheet 2 as the basis for improvements in COG as this design resulted in the minimum COG per dose value.

The process parameters varied in this analysis were the transduction efficiency and electroporation efficiency. These parameters were chosen because they were identified as key economic drivers by the sensitivity analysis. Furthermore, both viral transduction technologies and mRNA plasmids used in electroporation have seen rapid advances in recent years and it is feasible that further improvements in the efficiencies observed in these unit operations could be achieved.

Additionally, the cost of viral transduction per lot was tested in the scenario analyses, as was the capacity (in terms of number of cells) of purification platforms. Again, these were shown to be key economic drivers in the sensitivity analysis (Section 4.3). The price to the cell therapy manufacturer in this instance is negotiated with a contract manufacturing organisation (CMO) that is assumed to produce the viral vector used in the transduction stage of the bioprocess. This results in a 'viral transduction cost per lot'. As with other bioprocess sectors (not least the cell therapy field), advances in the technologies and reagents used in the production of viral vectors are being made. This is likely to result in reduced COG for the CMOs producing viral vectors; it is therefore not unreasonable to assume that cell therapy manufacturers will put pressure on these CMOs to reduce the selling price to reflect this. Thus, the cost of viral transduction may be reduced.

Purification technologies are limited in capacity and throughput; this has been the subject of many commentaries and reviews within the cell therapy bioprocess field [14,27]. As competition amongst manufacturers of purification platforms increases, and as demand from the process sector increases, it is likely that the capacities of these technologies will increase.

Having explored whether current processes can meet a cost target of COG as 15% TSP earlier (Fig. 3, Section 4.2), further scenarios were then carried out to see how much better the performance would need to be if the target was COG had to be even lower, set at 10% TSP. Fig. 8a indicates that viral transduction efficiency must be increased to 90% from 70%, along with a 22% increase in the purification capacity from the base case scenario, in order to achieve a COG as 10% TSP (Point B, Fig. 8a). Alternatively, a 50% increase in purification capacity and a minor increase in viral transduction efficiency to 73% could achieve this target (Point A, Fig. 8a).

This is a similar scenario to that where both reductions in the viral transduction cost per lot, and the viral transduction efficiency are varied. Point A in Fig. 8b illustrates that a reduction in viral transduction costs per lot of 38% is required, assuming viral transduction efficiency remains at the base case value. However, as shown by Point B in Fig. 8b, improvements in viral transduction costs alone are not sufficient to achieve COG equal to 10% of TSP. Furthermore, when both viral transduction and electroporation efficiencies are varied (Fig. 8c), when electroporation efficiency is increased to 84%, viral transduction efficiency is required to be 90% for COG equal to 10% of TSP to be achieved.

Fig. 8b and c indicate that significant process improvements are required in order to reach COG values equal to 10% of TSP, particularly if the capacity of purification platforms were to remain unchanged. Therefore, to analyse whether an increase in process capacity at the purification stage would have an effect on the required process improvements in other areas in order to achieve COG equal to 10% of TSP, the scenarios described by Fig. 8b and c were re-run under the assumption that the capacity of the purification technology had increased by 25% (Fig. 8d & e). Direct cost fluctuations that would be associated with this increased purification technology capacity were also considered in COG computations.
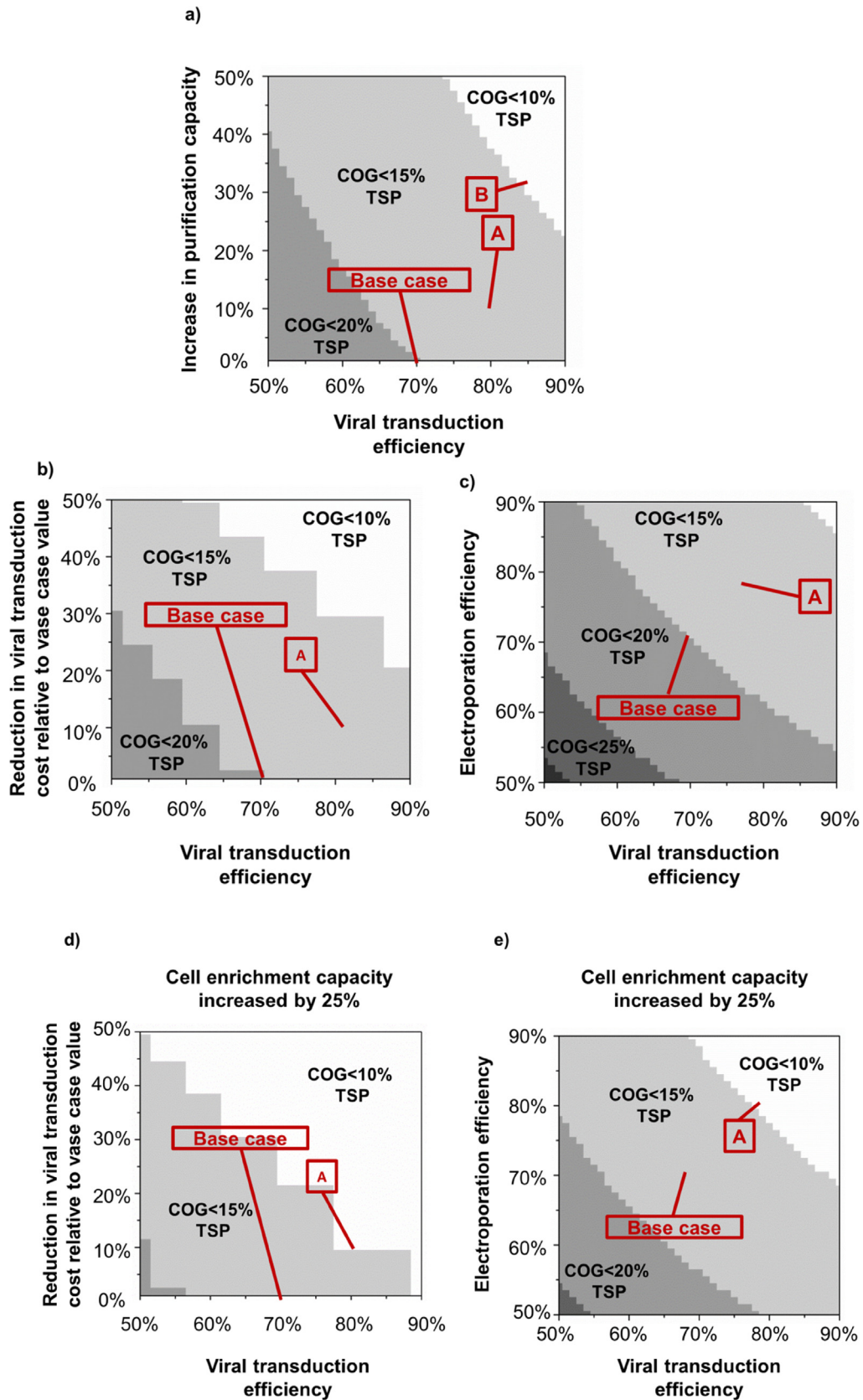
Fig. 8. Contour plots showing the windows of operations whereby COG values of below 15% of target selling price (TSP) can be achieved. Plot **a)** considers viral transduction efficiency and purification capacity (in terms of number of cells); Point A illustrates the bioprocess performance whereby COG is safely below 15% of TSP, Point B illustrates the bioprocess performance whereby COG is ~10% of TSP. Plots **b) & d)** consider viral transduction cost per lot and viral transduction efficiency are considered in one scenario. Plots **c) & e)** consider viral transduction efficiency and electroporation efficiency. Plots **b) & c)** consider scenarios where the capacity of purification technology remains at the base case value. Point A on the respective plots indicates the required bioprocess performance whereby COG is safely below 15% of TSP. Plots **d) & e)** consider scenarios where the capacity of purification technology is assumed to be 25% greater than the base case scenario. Here contour plots show required bioprocess performance whereby COG = ~10% of TSP (Point A on the respective plots). TSP was estimated to be US$50,000.

Table 6
Decision matrix for the evaluation of different process designs.

Attribute	Original rating data				Feasible Range	
	Flowsheet 1	Flowsheet 2	Flowsheet 3	Flowsheet 4	Worst Value	Best Value
COG per gram	7,829	7,630	8,220	7,888	9,500	6,500
FCI	932,574	556,797	703,097	623,397	500,000	1000,000
Process control	Tr(6.8, 7.3, 7.8)	Tr(6.8, 7.3, 7.8)	Tr(5.5, 6.0, 9.5)	Tr(5.2, 5.7, 6.2)	0	10
Process containment	Tr(8.2, 8.7, 9.2)	Tr(8.2, 8.7, 9.2)	Tr(8.5, 9.0, 9.5)	Tr(5.5, 6.0, 6.5)	0	10
Ease of scale-up	Tr(6.5, 7.0, 7.5)	Tr(5.8, 6.3, 6.8)	Tr(6.0, 6.5, 7.0)	Tr(5.0, 5.5, 6.0)	0	10
Ease of operation	Tr(6.2, 6.7, 7.2)	Tr(6.8, 7.3, 7.8)	Tr(6.5, 7.0, 7.5)	Tr(7.8, 8.3, 8.8)	0	10
Validation effort	Tr(6.5, 7.0, 7.5)	Tr(6.2, 6.7, 7.2)	Tr(5.5, 6.0, 6.5)	Tr(5.2, 5.7, 6.2)	0	10

Tr(a, b, c) refers to the triangular probability distribution where a, b, c are the minimum, most likely, and maximum values, respectively.

Fig. 8d illustrates that if a 25% increase in purification technology capacity is assumed, then a 21% reduction in the viral transduction cost per lot will result in COG equal to ~10% of TSP (Point A, Fig. 8d). Furthermore, if viral transduction costs can be improved from 70% to 88% then COG equal to 10% of TSP can be achieved (Point B, Fig. 8d). If the capacity of purification platforms improved by 25%, electroporation efficiency must be improved from 70% to 89% to achieve COG equal to ~10% of TSP (Point B, Fig. 8a).

The scenario analyses in this section offer evidence that allogeneic CAR-T cell therapies can achieve COG values as a percentage of target selling price similar to early biopharmaceutical products. They also illustrate how COG of 10% of TSP may be achieved. Depending on what are deemed to be the most feasible or achievable process improvements, the window of operation will be directed towards different regions of the contour plots. For instance, if viral transduction efficiency can be easily improved then process engineers may target Point B in Fig. 8a–e, however if improvements in other parameters prove more feasible, then a window of operation whereby COG ≈ 10% of sales close to Point A in Fig. 8a–e may be targeted. However, at this time in development, it must be emphasized that both COG and TSP are not definitively known as there as currently no examples of marketed allogeneic T cell therapies, and as such, the model should be used as a tool to determine the relative importance of altering various process parameters on COG.

In order to reduce COG, it is likely that improvements in current process technologies will be required (Fig. 8a, d & e). Previous case studies and reviews have commented on the lack of scalable, high resolution purification (sometimes referred to as purification) platforms [14,27]. The scenario analyses above indicate that improvements in this area of cell therapy bioprocesses, alongside the maximisation of potential yields of target cell types via the improvement of vector delivery systems, are key to reducing the COG burden associated with allogeneic cell therapy bioprocessing.

4.5. Multi attribute decision making analysis under uncertainty

MADM analysis was applied in this case study in order to evaluate potential process designs on the basis not only of financial attributes, but also operational attributes. In this case study, the use of MADM proved particularly instructive due to fact that the four top-ranked process flowsheets from a COG perspective all resulted in COG values within 10% of the optimal solution. MADM analysis was therefore used to select between different process designs in this instance. A stochastic MADM analysis was applied to Flowsheets 1, 2, 3 & 4, as defined in Section 3.2.

Uncertainty data was incorporated into the ratings given to the qualitative operational attributes for each technology by assigning appropriate probability distributions. Trular distributions were assigned to each attribute for each flowsheet, to represent their minimum, most likely, and maximum values. The resultant decision matrix for the evaluation of the four bioprocess flowsheets is therefore shown in Table 6.

Table 7
Summary of weighted dimensionless ratings for each attribute and process flowsheet tested within the MADM analysis.

| Parameter	Flowsheet			
	1	2	3	4
COG per dose	75	84	58	73
Fixed capital investment	5	40	26	34
Ease of operation	22	25	23	28
Process control	63	63	50	47
Validation effort	10	9	8	8
Ease of scale-up	37	32	34	28
Process containment	60	60	62	39

4.5.1. Qualitative operational benefits

Table 7 contains the mean dimensionless ratings scored by each process flowsheet for each attribute when evaluated using the stochastic MADM analysis. The data contained within Table 7 indicates that Flowsheet 3 ranks highest for process control amongst the four flowsheets. This is due to the integrated process platform's ability to run both concentration and purification unit operations within a controlled environment in an automated manner. This attribute was ranked the most important amongst respondents to a survey sent to bioprocess professionals. Process containment, referring to a bioprocess' ability to run without exposure to the surrounding environment was also ranked high in terms of its importance amongst operational attributes. Flowsheets 1–3 all achieved high ratings amongst respondents for this attribute. Table 7 shows that Flowsheets 1–3 containing rocking motion bioreactors were rated favourably compared to Flowsheet 4, containing gas-permeable vessels, for all operational attributes aside from ease of operation. This is due to the automated media removal device used for media exchanges associated with gas-permeable vessels as opposed to complex perfusion culture strategies used within the rocking motion bioreactor platform. In order to test whether the operational benefits associated with Flowsheets 1 and 3 outweigh the high score achieved for the FCI attribute achieved by Flowsheet 4, it was necessary to consider the aggregate scores achieved by each process flowsheet in the MADM analysis.

4.5.2. Multi-attribute decision making analysis under uncertainty

The cumulative frequency distribution of the aggregate score of the alternative process flowsheets was generated and is displayed in Fig. 9. Initially, equal importance of operational and financial attributes was assumed (i.e. $R_1 = R_2 = 0.5$). The cumulative frequency curves for Flowsheets 2 and 4 do not intersect with each other, or any other curves on the chart. However, Flowsheets 1 and 3 intersect with one another just above the median value. Flowsheet 1 achieved a preferable aggregate score compared to Flowsheet 3 in 51% of Monte Carlo simulations. Flowsheet 3 also resulted in the greater range of values compared to Flowsheet 1. This indicates that the uncertainty associated with Flowsheet 3 is greater than Flowsheet 1, and therefore whilst the median aggregate scores are approximately equal, it may be that Flowsheet 1 is considered
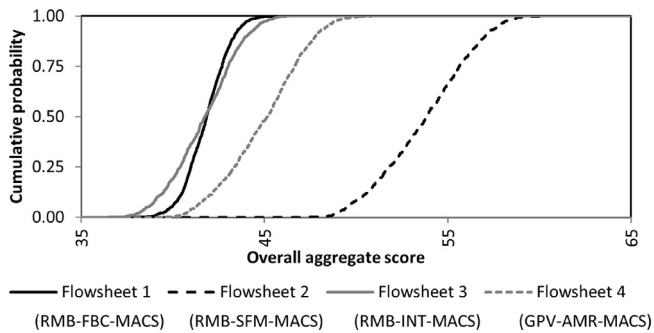
Fig. 9. Cumulative frequency curves showing the spread of aggregate scores as computed by the MADM component of the tool. Aggregate scores were generated over 1000 Monte Carlo simulations.
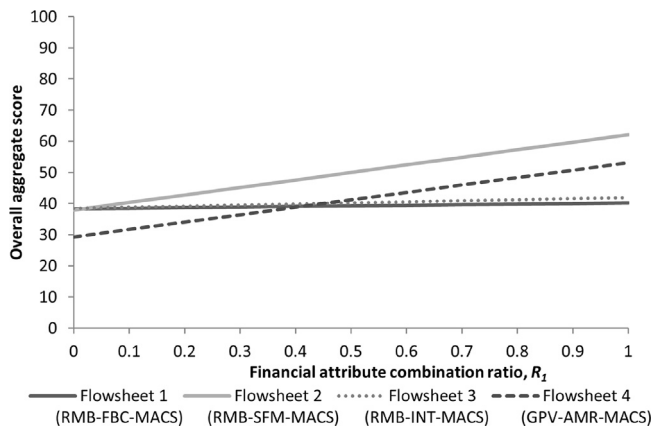
Fig. 10. Spider plots showing depicting the sensitivity of the overall aggregate MADM score for each flowsheet design to variations in the financial attribute combination ratio, or the importance given to financial attributes within the MADM analysis. The sum financial attribute combination ratio (R_1) and operational attribute combination ratio (R_2) (not shown on chart) are always equal to 1. The technologies used in each flowsheet deign are provided in Table 5.

preferable to Flowsheet 3 due to the reduction in variability of its aggregate score. Flowsheet 2 is clearly the preferred alternative of all the options presented in Fig. 9. It is therefore possible to rank the alternatives in order of preference; Flowsheet 2, Flowsheet 4, Flowsheet 1, Flowsheet 3.

4.5.3. Multi-attribute decision making analysis: sensitivity to financial and operational weightings

The results of reconciling trade-offs between financial and operational outputs using a single multi-attribute score are discussed in this section. Previous sections of this work have focused on identification of the preferred process design when operational and financial attributes were given equal ratings. Here, overall strategy scores were calculated for each process design using MADM analysis across a range of combination ratios. These combination ratios reflect the relative importance of financial and operational attributes in process design. The financial combination ratio, R_1, and the operational attribute combination ratio, R_2 were assigned such that $R_1 + R_2 = 1$ under any circumstance. Therefore if one combination ratio is varied, the other is adjusted to reflect this change.

In this instance, the weightings assigned to each individual attribute were kept constant and were not subject to uncertainty. The average weightings assigned to each attribute during the Monte Carlo simulation, shown in Table 1, were applied for the purposes of this deterministic analysis.

The combination ratios were then assigned a values ranging from 0 to 1 (at intervals of 0.1). Fig. 10 depicts the sensitivity of the overall aggregate score for each flowsheet to the finan-

cial and operational combination ratios at an annual demand of 1000 dose per year and a dose size of 10^8 target cells per dose. If the operational attributes are considered approximately twice as important as the financial attributes ($R_2 = 0.65$, $R_1 = 0.35$), Flowsheet 4 is ranked bottom of the four flowsheets tested using MADM. However, when financial attributes are considered at least as important as economic attributes ($R_1 = R_2 = 0.5$), Flowsheet 4 is ranked above Flowsheets 1 and 3, despite all flowsheets obtaining a similar ranking for COG per dose. Flowsheet 4 is ranked favourably to Flowsheets 1 & 3 due to its superior FCI ranking; the gas-permeable vessel technology is characterised by low FCI costs. Flowsheets 1 & 3 are ranked approximately equally across scenarios tested; they scored similarly in both economic and operational categories. Flowsheet 3 is favoured slightly owing to the greater process containment offered by this strategy, and a reduction in FCI costs. Indeed in scenarios where operational attributes are considered 9 times (or greater) the importance of economic attributes, Flowsheet 3 is the top ranked technology, although the difference between the aggregate scores for Flowsheets 1, 2 and 3 in these instances are not significant. Flowsheet 2 is the top ranked flowsheet in all other scenarios tested; it offers significant operational and economic benefits in comparison to Flowsheet 4 due to the process containment and process control offered by rocking motion bioreactors. The FCI rating for Flowsheet 3 is also significantly higher than Flowsheets 1 and 2, due to the relatively low cost of the spinning membrane filtration technology, as opposed to fluidised bed centrifuge or the integrated process platform, used for cell concentration.

5. Conclusion

A case study has been presented whereby a decisional tool, consisting of a bioprocess economics model, information database and MADM analysis has been developed in order to facilitate decision making with regards to process design for an allogeneic CAR-T cell manufacturing process. Cost-effective equipment sizing regimes were identified for alternative process flowsheets. Flowsheets consisted of a variety of different technology platforms to support cell culture, concentration of cells, and enrichment of target cell populations. The difference in COG values of three of the process designs evaluated within the study did not exceed 10% compared to the most cost-effective design (in terms of COG per dose). It was found that using tissue culture plastic culture ware such as T-flasks and multilayer vessels proved to be significantly more costly than rocking motion bioreactors or gas permeable vessels. A sensitivity analyses indicated that viral transduction efficiency, electroporation efficiency, viral transduction cost per lot and the capacity of downstream processing equipment (in terms of cell numbers) were the key process economic drivers; improvements required to bring about a COG per dose value significantly below 15% of target selling price were subsequently identified using scenario analyses. MADM analysis was also able to identify that the flowsheet consisting of rocking motion bioreactor, spinning filter membrane, and a standalone MACS platform as the preferred process design when both financial and operational attributes were taken into account. Future work is considering comparisons between allogeneic and autologous CAR-T cell COG in order to identify scenarios whereby one product type is more economically viable than the other. Other avenues for future work include extending the sensitivity scenarios with stochastic modelling, such as Monte Carlo simulations, to capture the impact on the process robustness [13,17,20] as well as capturing the impact of regional differences in regulatory requirements (e.g. for cleanroom environments) on the manufacturing costs.

Acknowledgments

References

[1] A.D. Kaiser, M. Assenmacher, B. Schröder, M. Meyer, R. Orentas, U. Bethke, B. Dropulic, Towards a commercial process for the manufacture of genetically modified t cells for therapy, Cancer Gene Ther. 22 (2015) 72–78, http://dx.doi.org/10.1038/cgt.2014.78.

[2] B.L. Levine, Performance-enhancing drugs: design and production of redirected chimeric antigen receptor (CAR) T cells, Cancer Gene Ther. 22 (2015) 79–84, http://dx.doi.org/10.1038/cgt.2015.5.

[3] B.L. Levine, J. Miskin, K. Wonnacott, C. Keir, Global manufacturing of CAR T cell therapy, Mol. Ther. Methods Clin. Dev. 4 (2017) 92–101, http://dx.doi.org/10.1016/j.omtm.2016.12.006.

[4] J. Valton, V. Guyot, A. Marechal, J.-M. Filhol, A. Juillerat, A. Duclert, P. Duchateau, L. Poirot, A multidrug-resistant engineered CAR T cell for allogeneic combination immunotherapy, Mol. Ther. 23 (2015) 1507–1518, http://dx.doi.org/10.1038/mt.2015.104.

[5] R. Pierson, Safety concerns cloud early promise of powerful new cancer drugs, Reuters. (2015).

[6] A. Walker, R. Johnson, Commercialization of cellular immunotherapies for cancer, Biochem. Soc. Trans. 44 (2016) 329, LP–332.

[7] R. Hettle, M. Corbett, S. Hinde, R. Hodgson, J. Jones-Diette, N. Woolacott, S. Palmer, The assessment and appraisal of regenerative medicines and cell therapy products: an exploration of methods for review, economic evaluation and appraisal, Health Technol. Assess. (Rockv.) 21 (2017) 1–204, http://dx.doi.org/10.3310/hta21070.

[8] J. Hartmann, M. Schüßler-lenz, A. Bondanza, C.J. Buchholz, Clinical Development of CAR T Cells — Challenges and Opportunities in Translating Innovative Treatment Concepts, 9, 2017, pp. 1183–1197, http://dx.doi.org/10.15252/emmm.201607485.

[9] C. Wegener, Cell washing with the LOVO cell processing system, Bioprocess. Int. (August) (2014) 78.

[10] Sartorius Stedim, Scalable Single-Use Centrifugation Systems, 2016.

[11] J.F. Vera, L.J. Brenner, U. Gerdemann, M.C. Ngo, U. Sili, H. Liu, J. Wilson, G. Dotti, H.E. Heslop, A.M. Leen, C.M. Rooney, Accelerated production of antigen-specific T cells for preclinical and clinical applications using gas-permeable rapid expansion cultureware (G-Rex), J. Immunother. 33 (2010) 305–315, http://dx.doi.org/10.1097/CJI.0b013e3181c0c3cb.

[12] C.L. Darkins, C.-F. Mandenius, Design of large-scale manufacturing of induced pluripotent stem cell derived cardiomyocytes, Chem. Eng. Res. Des. 92 (2013) 1–11, http://dx.doi.org/10.1016/j.cherd.2013.08.021.

[13] M. Jenkins, J. Bilsland, T.E. Allsopp, S.V. Ho, S.S. Farid, Patient-specific hiPSC bioprocessing for drug screening: bioprocess economics and optimisation, Biochem. Eng. J. (2015).

[14] B.D. Weil, M.J. Jenkins, S. Uddin, D.G. Bracewell, S.S. Farid, F.S. Veraitch, An integrated experimental and economic evaluation of cell therapy affinity purification technologies, Regen. Med. 12 (2017) 397–417, http://dx.doi.org/10.2217/rme-2016-0156.

[15] A.S. Simaria, S. Hassan, H. Varadaraju, J. Rowley, K. Warren, P. Vanek, S.S. Farid, Allogeneic cell therapy bioprocess economics and optimization: single-use cell expansion technologies, Biotechnol. Bioeng. 111 (2014) 69–83, http://dx.doi.org/10.1002/bit.25008.

[16] T.D. Pereira Chilima, T. Bovy, S.S. Farid, Designing the optimal manufacturing strategy for an adherent allogeneic cell therapy, Bioprocess. Int. 14 (2016) 24–31.

[17] S. Hassan, A.S. Simaria, H. Varadaraju, S. Gupta, K. Warren, S.S. Farid, Allogeneic cell therapy bioprocess economics and optimization: downstream processing decisions, Regen. Med. 10 (2015) 591–609 http://www.futuremedicine.com/doi/pdf/10.2217/rme.15.29?src=recsys.

[18] S. Hassan, H. Huang, D. Smith, Process change evaluation framework for allogeneic cell therapies : impact on drug development and commercialization, Regen. Med. 11 (2016) 287–305.

[19] K.P. Yoon, C. Hwang, Multiple Attribute Decision Making, 1995, http://dx.doi.org/10.4135/9781412985161.

[20] S.S. Farid, J. Washbrook, N.J. Titchener-Hooker, Decision-support tool for assessing biomanufacturing strategies under uncertainty: stainless steel versus disposable equipment for clinical trial material preparation, Biotechnol. Prog. 21 (2005) 486–497, http://dx.doi.org/10.1021/bp049692b.

[21] J. Pollock, S.V. Ho, S.S. Farid, Fed-batch and perfusion culture processes: economic, environmental, and operational feasibility under uncertainty, Biotechnol. Bioeng. 110 (2013) 206–219, http://dx.doi.org/10.1002/bit.24608.

[22] S.S. Farid, A Decision-Support Tool for Simulating the Process and Business Perspectives of Biopharmaceutical Manufacture, University College London, 2002.

[23] S. Yang, S.A. Rosenberg, R.A. Morgan, Clinical-scale lentiviral vector transduction of PBL for TCR gene therapy and potential for expression in less-differentiated cells, J. Immunother. 31 (2008) 830–839, http://dx.doi.org/10.1097/CJI.0b013e31818817c5.

[24] R. Maciulaitis, L. D'Apote, A. Buchanan, L. Pioppo, C.K. Schneider, Clinical development of advanced therapy medicinal products in Europe: evidence that regulators must be proactive, Mol. Ther. 20 (2012) 479–482.

[25] C.A. Bravery, Are biosimilar cell therapy products possible? Innov. Cell. Tissue Biother. Marseille Fr. (2012) http://advbiols.com/documents/Bravery-AreBiosimilarCellTherapiesPossible.pdf.

[26] D.M. Smith, Assessing commercial opportunities for autologous and allogeneic cell-based products, Regen. Med. 7 (2012) 721–732, http://dx.doi.org/10.2217/rme.12.40.

[27] B.D. Weil, F.S. Veraitch, Bioprocessing challenges associated with the purificaiton of cellular therapies, in: Stem Cells Cell Ther., 2013, pp. 293–326, http://dx.doi.org/10.1007/978-3-319-02904-7.